

**Military Technical College  
Kobry El-Kobbah,  
Cairo, Egypt**



**9<sup>th</sup> International Conference  
on Civil and Architecture  
Engineering  
ICCAE-9-2012**

## **CREEP PREDICTION OF SELF-CONSOLIDATING CONCRETE INCORPORATING CLASS-F FLY ASH**

**I. Adam<sup>1</sup> and M. M. Reda Taha<sup>2</sup>**

### **ABSTRACT**

Self-consolidating concrete (SCC) is a relatively new type of concrete with a number of attractive properties, particularly in its fresh state. In spite of the extensive research studies carried out on SCC in the last two decades, its time-dependent behavior including creep and shrinkage has not received ample attention. This paper presents the results of an experimental investigation aiming to identify creep (under compressive stresses) of SCC containing class-F fly ash. In this work three different SCC mixes were prepared to investigate the effect of changing levels of fly ash on creep of SCC. The adopted fly ash contents were 20%, 40%, and 60%, by mass, of the total binder materials content (cement plus fly ash). The water/binder ratios of the SCC mixes were kept constant at 0.33 and the total binder content was kept at fixed value of 450 kg/m<sup>3</sup>. Experimental results were compared with the popular ACI and CEB-FIP prediction models for creep in concrete in order to compare the creep of SCC mixes to that of Normally-Vibrated Concrete (NVC). Due to the ACI model's dependence on knowing the slump of the concrete, the authors propose a change in the model. The comparison of experimental results with the CEB-FIP models suggests that creep compliance of SCC mixes containing fly ash is significantly higher than that of NVC.

### **KEYWORDS:**

Self-Consolidating Concrete, Creep, Shrinkage, Fly ash

### **RESEARCH SIGNIFICANCE**

Self-consolidating concrete (SCC) is a relatively new type of concrete defined by significantly enhanced fresh properties eliminating the need of vibration or any type of mechanical compaction. SCC is characterized by its ability to flow through structural elements under its own weight and fill every corner of formwork even in the presence of congested steel reinforcement. Therefore, SCC represents one of the most outstanding advances in the field of concrete technology. Over the past few decades many researchers have examined the fresh and hardened properties of SCC, however long-term properties such as creep and shrinkage have not received sufficient attention. To add to the understanding of the creep of SCC, an experimental program was carried out at the University of New Mexico where three SCC mixes containing variable amounts of class-F fly ash were subjected to sustained compressive stresses.

1 Associate Professor, Construction Research Institute, National Water Research Center, Delta Barrage, Egypt.

2 Associate Professor & Regents' Lecturer, Dept. of Civil Engineering, Univ. of New Mexico, Albuquerque, NM, USA.

The results of this experimental program were compared to the popular ACI and CEB creep models in order to compare the creep of these concrete mixes to that of normal vibrated concrete (NVC). Since the ACI model depends on knowing the slump of the fresh concrete the authors propose a modification allowing the modeling of creep of SCCs containing class-F fly ash.

## INTRODUCTION

Since its breakthrough in the late 1980s (Ozawa, Neakawa et al. 1989), SCC has gained considerable momentum and has been applied successfully to numerous bridges and structures (Domone 2007). Numerous studies have been carried out to examine the fundamental properties of SCC and the influence of its constituents on its fresh and hardened properties such as flowability, passing ability, segregation resistance, strength, and durability characteristics (Bouzoubaa and Lachemi 2001; Domone 2005; Khatib 2008, Sahmaran, Yaman et al. 2009, Khayat and Long 2010, Adam 2011(a), Adam 2011(b)). There have also been several regional and international conferences held focusing on the use and applications of SCC in the last couple of decades. The significant enhancement in workability and segregation resistance of SCC is achieved through the inclusion of large amounts of fine particles and viscosity modifying agents (Brouwers and Radix 2005). The enhancement in SCC microstructure is reflected on improved properties of hardened SCC such as strength, bond to steel reinforcement, and durability.

Existing literature reports conflicting findings on creep of SCC in comparison with NVC. Persson (Persson 2005) examined the creep of SCC and NVC mixes with varying w/cm ratios, stress to strength levels, and loading ages using traditional spring loading devices. From these experiments it was found that the SCC mixes loaded both young and mature exhibited creep similar to that of NVC mixes of similar strength. It was also found that creep of both SCC and NVC mixes increased at a similar rate when the specimens were loaded at younger ages. Seng and Shima (Seng and Shima 2005) compared creep of SCC mixes with varying limestone filler contents to a control NVC mix. While creep was shown to increase with increasing limestone content, creep of SCC was comparable to NVC. Similar findings were reported by Collepardi et al. (Collepardi 2005) for SCC mixes containing limestone powder. Sukumar et al. (Sukumar, Nagamani et al. 2008) reported SCC incorporating fly ash and VMA to experience less total creep strain in comparison with NVC specimens.

On the other hand, Heirman et al. (Heirman, Vandewalle et al. 2008) reported powder type SCC mixes incorporating a limestone powder as mineral filler to show higher creep in comparison with a control NVC. However, the CEB-FIP Model Code (MC-90) was shown to be able to predict the creep of these powder type SCCs accurately. Reinhardt et al. (Reinhardt, Adam et al. 2008) investigated total and basic creep of a VMA type SCC mixes containing variable amounts of fly ash as a partial replacement of cement. This investigation showed creep compliance of SCC mixes to increase with increasing amounts of fly ash replacement. Furthermore, SCC mixes exhibited a higher amount of creep compliance in comparison with a control NVC mix containing no fly ash. Collepardi et al. (Collepardi 2005) also reported SCC mix containing fly ash exhibited higher creep in comparison. This

was attributed to unreacted fly ash which was thought to be deformed upon specimen loading. Mazzotti and Ceccoli (Mazzotti and Ceccoli 2008) investigated creep of SCC mixes with different types and varying amounts of cement and a fixed dosage of a combine super plasticizer and VMA. Attempting to model the results of these experiments with the CEB-FIP MC90 creep model showed the model to underestimate creep of these SCC mixes by about 30 to 60%. To account for this, authors proposed a modification factor based on the cement to lime stone powder ratio for accurate creep modeling.

Other research programs investigated the effects of powder content, VMA type, and cement amount and type on the creep of SCC. Lowke and Schießl (Lowke and Schießl 2008) investigated the effect of powder content and VMAs on the creep SCC mixes. The results showed creep of SCC was not significantly affected by the type of VMA used. However, it was shown that an increase in air voids due to adding air-entrainment increased creep of SCC significantly. It was also found that the SCC mixes with the lower limestone powder content exhibited higher creep in comparison with the SCC mixes containing high limestone content. In fact, the reduction of limestone powder also resulted in a coarser pore structure which appeared to favor creep (Lowke and Schießl 2008). Maia et al. (Maia, Nunes et al. 2008) investigated creep and shrinkage of SCC mixes containing high, medium and low paste contents. All three SCC mixes contained Portland cement, limestone filler, superplasticizer, two types (fine and coarse) of siliceous sand, and coarse crushed stone granite. It was reported that SCC with low paste content exhibited the highest creep when loaded at 24 hours. However, the different mixes did not exhibit a significant difference in creep from the control specimens when loaded at 3 and 7 days.

## **EXPERIMENTAL METHODS**

### **Materials and Mix Proportions**

Three SCC mixes incorporating fly ash as a partial replacement for cement content were prepared. The fly ash contents were 20%, 40%, and 60%, by mass, of the total cementitious materials content. Superplasticizer (SP) and viscosity modifying admixture (VMA) doses were adjusted in order to maintain the same amount of flowability for each of the three SCC mixes. The water/binder (cement plus fly ash) ratios of the SCC mixes were kept constant at 0.33 and the total cementitious content was kept at fixed at 450 kg/m<sup>3</sup>. The mix proportions of the three concrete mixes are summarized in Table 1.

### **Fresh and Hardened Concrete Properties**

Upon completion of a standard mixing procedure, fresh concrete properties were evaluated. Concrete flowability and passability was determined using the slump flow and passing ability tests. Both tests were conducted according to European Guidelines for SCC (European Self-Compacting Concrete Group 2005). The slump flow test was used to measure the flowability and the viscosity of SCC mixes. T<sub>500</sub> represents the time it took the concrete to flow over a 500 mm diameter circle from the slump cone. The passability test was performed using a standard L-box device. Table 2 shows the fresh properties of the three different concrete mixes. It is important to mentioning that there were no visual signs of bleeding or segregation during testing of all SCC mixes in the fresh state. Moreover, aggregate particles were

suspended within the mixes and were present all the way to the perimeter with no indication of mortar separation at the circumference of the concrete flow. Table 3 gives the hardened concrete compressive strength values at both 7 and 28 days for all investigated SCC mixes.

### **Specimens and Specimen Preparation**

After discerning the fresh properties, the concrete was cast into a total of four compression creep and shrinkage prismatic specimens of 100 x 100 mm cross-section and 400 mm length. Fresh concrete was also cast into cylinders, 100 mm diameter by 200 mm in length, used for obtaining concrete compressive strength with time. Standard ASTM procedures were followed in preparing the concrete specimens (ASTM C192 2007). Specimens for compression creep experiments were cast with a 25 mm inner diameter centrally oriented PVC pipe extruding 12 mm from the concrete specimen end. All concrete specimens were allowed to harden for 24 hours before being removed from the molds. After being removed from the molds concrete specimens were placed in a temperature controlled ( $23\pm 2$  °C) lime-saturated water curing bath until the day of loading following ASTM standards for curing concrete (ASTM C192 2007). At 11 days of age concrete creep specimens were removed from the curing bath and allowed to air dry until they reached a surface dry condition. Four DEMEC disks were glued to two opposite surfaces of creep and shrinkage specimens. The disks were placed with a placement rod which achieved an initial gauge length of 250 mm.

### **Creep Experimental Setup**

Two 13 mm thick steel plates with a 25 mm diameter center bored holes were placed over the extruding PVC pipe on the specimen surfaces. An 18 mm diameter threaded steel rod was passed through the PVC pipe. Another pair of 13 mm thick steel plates with 18 mm diameter holes were slid over the steel rod and attached with two loosely tightened locking nuts and one washer on each end. The creep specimens were planned to be loaded in compression by tensioning the steel rods and locking them in place as in a concrete post-tensioning scheme. The creep specimen was then placed in a Tinius Olsen Universal Testing Machine (UTM). Then the steel rod was pre-tensioned to the desired load as shown in Figure 1. The load was held constant and the nuts were tightened securing the steel plates. The load was then released on the UTM transferring the load from the prestressing rod to the steel plates. This caused the steel plates to exert sustained compressive stresses on the concrete specimen. A force transfer schematic is shown in Figure 1. All compression creep specimens were subjected to a nominal stress of 35% of the concrete compressive strength measured at 7 days of age. Immediately after loading, the initial displacements were recorded. Due to stress relaxation in the steel rod and creep of concrete all creep specimens were re-stressed to the original stress after 1, 3, 15, 25 and 51 days after initial loading and every 56 days thereafter. This procedure for producing creep specimens was used following Adam (Adam 2003). Two specimens of each concrete mix (wrapped and unwrapped) were loaded to observe drying and basic creep.

Specimens were kept in the laboratory which was automatically controlled to maintain constant temperature ( $23\pm 2$  °C), while the relative humidity (RH) ranged from 40 to 75%. It is important to note that no thermal effects were considered in these experiments. Temperature variation within service conditions (similar to lab temperature here) of concrete proved to have insignificant effect on creep and shrinkage of concrete (Neville, Dilger et al.

1983). For each loaded (creep) specimen, an unloaded specimen was stored in the same environmental conditions for observing the shrinkage strains. Measurements of creep and shrinkage strains on sealed specimens were performed to enable separating the contribution of basic creep and shrinkage from the effect of drying creep and shrinkage, respectively. Creep and shrinkage observations were recorded at 1, 3, 7, 10, 14, 21, 28, 35, and 42 days and every 14 days thereafter.

Readings were taken on all specimens using a mechanical caliper manufactured by Mayes Instruments, Co.. This caliper is fitted with sharp conical reading points that fit precisely into predrilled holes in the attached DEMEC disks. The mechanical caliper takes readings with respect to a reference bar with a gauge length of 250 mm. DEMEC disks were placed with a placement bar manufactured to precisely fit the reference bar.

### EXPERIMENTAL ANALYSIS

Length measurements obtained from the mechanical caliper allowed for the calculation of displacement strain  $\epsilon$  (Equation 1).

$$\epsilon = \frac{L_t - L_{t0}}{L_{t0}} \quad (1)$$

Where  $L_t$  represents length measurements with time and  $L_{t0}$  represents the initial length measurement at time zero. Since elastic strain was recorded independently from the creep specimens upon loading,  $L_{t0}$  for creep specimens represents the measurement taken immediately after loading. Equations 2 and 3 present the strains measured on both loaded and unloaded specimens respectively.

$$\epsilon_{creep} = \epsilon_{bc} + \epsilon_{dc} + \epsilon_{bs} + \epsilon_{ds} \quad (2)$$

$$\epsilon_{shrinkage} = \epsilon_{bs} + \epsilon_{ds} \quad (3)$$

Where  $\epsilon_{creep}$  represents the total strain obtained from the loaded creep specimens and  $\epsilon_{shrinkage}$  represents the total strain obtained from unloaded shrinkage specimens. The individual components of creep and shrinkage are denoted as  $\epsilon_{dc}$  (strain due to drying creep),  $\epsilon_{bc}$  (strain due to basic creep),  $\epsilon_{ds}$  (strain due to drying shrinkage), and  $\epsilon_{bs}$  (strain due to basic shrinkage). Subtracting Equation 3 from Equation 2 enables isolating the creep strain components of drying and basic creep, which together represent total creep. Once the total creep strains were separated, the creep coefficient  $\phi(t, t_0)$  was calculated as the ratio between the creep strain developed with time and the elastic strain.

$$\phi(t, t_0) = \frac{\epsilon(t, t_0) - \epsilon(t_0)}{\epsilon(t_0)} \quad (4)$$

In Equation 4  $\epsilon(t, t_0)$  represents the total strain observed with time (sum of elastic strain and creep strain) and  $\epsilon(t_0)$  represents the elastic strain.

## EXPERIMENTAL MODELING

In an effort to relate the creep observed from SCC to that predicted by design codes for concretes with similar strength we compare the observed creep to creep predicted by two design codes. These are the creep predictions based on the American Concrete Institute (ACI) model ACI 209R-2002 and that by the European code (known to be the most accurate prediction model) the CEB-FIP model MC-90-99. Our selection of the ACI-209 and CEB-FIP models is attributed to the fact that both models are the two most used models for being recommended by the ACI and for the CEB-FIP being reported to have a significantly low coefficient of variation (< 29%).

### ACI 209R - 92 Creep Prediction Model

The ACI 209R – 92 model predicts the creep coefficient, which is defined by Equation 4 in the previous section. Equation 5 presents the ACI model for prediction of creep coefficient  $\phi(t, t_0)$ .

$$\phi(t, t_0) = \frac{(t-t_0)^\psi}{d + (t-t_0)^\psi} \phi_u \quad (5)$$

In Equation 5,  $t_0$  is the age of concrete at loading,  $t$  is the time of measuring creep  $\phi_u$  is the ultimate creep coefficient, and  $\psi$  and  $d$  are coefficients that depend on the shape and size of the member. The shape and size of the member be completely taken accounted for by setting  $\psi$  to 1.0 and representing  $d$  by

$$d = 26.0 e \left[ 1.42 \times 10^{-2} (V/S) \right] \quad (6)$$

where  $V/S$  represents the volume to surface ratio of the concrete member.

For standard conditions the ACI, recommends the ultimate creep coefficient  $\phi_u$  to be set at 2.35. For any other condition ACI recommends  $\phi_u$  be modified by a series of correction factors and be replaced with Equation 7.

$$\phi_u = 2.35 \gamma_c \quad (7)$$

Where  $\gamma_c$  (defined in Equation 8) is the cumulative product of a series of correction factors based on curing duration, relative humidity, volume to surface ratio, slump, ratio of fine to total aggregate, and air content.

$$\gamma_c = \gamma_{c,t_0} \gamma_{c,RH} \gamma_{c,vs} \gamma_{c,s} \gamma_{c,\omega} \gamma_{c,\alpha} \quad (8)$$

For time of load applications greater than 7 days  $\gamma_{c,t_0}$  for adjusting the ultimate creep is defined by

$$\gamma_{c,t_0} = 1.25t_0^{-0.118} \quad (209)$$

where  $t_0$  is the age of concrete loading in days. The factor to correct for relative humidity  $\gamma_{c,RH}$  is defined as

$$\gamma_{c,RH} = 1.27 - 0.67h \quad (10)$$

where  $h$  denotes relative humidity in decimals greater than 0.40 (ACI 209 recommends using a value of greater than 1 for a relative humidity less than 0.40). To correct for differences in volume to surface ratio Equation 11 is used.

$$\gamma_{c,vS} = \frac{2}{3} \left( 1 + 1.13 e^{[-0.0213(V/S)]} \right) \quad (11)$$

In Equation 11  $V/S$  represents the volume to surface ratio (represented in mm). The correction factor for the slump  $\gamma_{c,s}$  is define as

$$\gamma_{c,s} = 0.82 + 0.00264s \quad (12)$$

where  $s$  is the slump of the concrete represented in mm. The ratio of fine aggregate to total aggregate is corrected for with  $\gamma_{c,\omega}$  which is defined by Equation 13.

$$\gamma_{c,\omega} = 0.88 + 0.0024\omega \quad (13)$$

Where  $\omega$  is the ratio of the fine aggregate to total aggregate by weight as a percentage. Lastly, Equation 14 shows the air content factor  $\gamma_{c,\alpha}$  (ACI recommends a value not less than 1.0)

$$\gamma_{c,\alpha} = 0.46 + 0.09\alpha \quad (14)$$

where  $\alpha$  is the air content as a percentage.

There is clearly a need to modify the ACI-209 model in order to predict creep of SCC due to the model's dependence on knowing the concrete's slump (Equation 12). To predict the creep of SCC mixes using fly ash replacement, a coefficient based on the fly ash replacement percentage is proposed. We did not choose slump flow because different SCC mixes with the same slump flow can show vastly different compressive strength and creep. It should be noted here that many common parameters of the concrete mixes could be used (i.e. admixture content, water/binder ratio, volume of cement paste, etc.) However, in our case fly ash replacement had the most significant effect on compressive strength and creep (Adam et al. 2007). This coefficient was found by fitting the ACI-209 model to our experimental data by optimizing the coefficient to minimize the root mean squared error (RMSE) between the

predicted model's and the experiment's ultimate creep coefficient. A relationship was then found using least squares method to relate each modified slump coefficient obtained for each concrete to that concrete's fly ash replacement percentage. The result is a new coefficient to replace the slump coefficient for SCC mixes. This new coefficient is defined as

$$\gamma_{c,s} = \begin{cases} 1 + 0.0006F^2 - 0.0015F & 0 \leq F \leq 40 \\ 2.0 & 40 \leq F \leq 60 \end{cases} \quad (15)$$

where F is the fly ash replacement ratio represented as a percentage.

### CEB MC90 – 99 Creep Prediction Model

The CEB MC90 – 99 Creep model also predicts creep of concrete in terms of creep coefficient. This model does not predict creep coefficient for instances where the stress to mean concrete strength at the time of loading is more than 40%. For this model the creep coefficient  $\phi(t, t_0)$  can be calculated from Equation 16

$$\phi_{28}(t, t_0) = \phi_0 \beta_c(t - t_0) \quad (16)$$

where  $\phi_0$  is the notional creep coefficient and  $\beta_c(t - t_0)$  is a coefficient that describes the development of creep with time. The notional creep coefficient can be determined using Equations 17 through 22.

$$\phi_0 = \phi_{RH} \beta(f_{cm28}) \beta(t_0) \quad (17)$$

$$\phi_{RH} = \left[ 1 + \frac{1 - h/h_0}{\sqrt[3]{0.1[(V/S)/(V/S)_0]}} \alpha_1 \right] \alpha_3 \quad (18)$$

$$\beta(f_{cm28}) = \frac{5.3}{\sqrt{f_{cm28}/f_{cmo}}} \quad (19)$$

$$\beta(t_0) = \frac{1}{0.1 + (t_0/t_1)^{0.2}} \quad (20)$$

$$\alpha_1 = \left[ \frac{3.5 f_{cmo}}{f_{cm28}} \right]^{0.7} \quad (21)$$

$$\alpha_2 = \left[ \frac{3.5 f_{cmo}}{f_{cm28}} \right]^{0.2} \quad (22)$$

Where  $f_{cm28}$  is the mean compressive strength of standard concrete cylinder at 28 days represented in MPa,  $f_{cmo}$  equals 10 MPa,  $h$  is the relative humidity of the ambient environment in decimals,  $h_0$  equals 1,  $V/S$  is the volume to surface ratio represented in mm,

$(V/S)_0$  equals 50 mm,  $t_1$  is 1 day, and  $t_0$  represents the age of concrete at loading adjusted by Equation (23) to account for the effect of cement type on the creep coefficient.

$$t_0 = t_{0,T} \left[ \frac{9}{2 + (t_{0,T}/t_{1,T})^{1.2}} + 1 \right]^\alpha \quad (23)$$

In Equation 23  $t_{0,T}$  is the concrete age at loading for a temperature equal to 20°C (needs to be adjusted for other temperatures),  $t_{1,T}$  equals 1 day, and  $\alpha$  is a coefficient depending on the type of cement ( $\alpha = 0$  for normal cement).

The coefficient  $\beta_c(t - t_0)$  that describes the development of creep with time may be determined from Equations 24, 25, and 26.

$$\beta_c(t-t_0) = \left[ \frac{(t-t_0)/t_1}{\beta_H + (t-t_0)/t_1} \right]^{0.3} \quad (24)$$

$$\beta_H = 150 \left[ 1 + (1.2 \cdot h/h_0)^{18} \right] (V/S)/(V/S)_0 + \alpha_3 \leq 1500\alpha_3 \quad (25)$$

$$\alpha_3 = \left[ \frac{3.5 f_{cm0}}{f_{cm28}} \right]^{0.5} \quad (26)$$

where  $(t - t_0)$  is the duration of the creep loading in days,  $t_1$  equals 1day,  $V/S$  is the volume to surface ratio represented in mm.  $(V/S)_0$  equals 50 mm,  $h$  is the relative humidity of the ambient environment in decimals,  $h_0$  equals 1,  $f_{cm28}$  is the mean compressive strength of standard concrete cylinder at 28 days measured in MPa, and  $f_{cm0}$  equals 10 MPa.

To compare the predicted results of the ACI and CEB-FIB creep prediction models, the root mean square error (RMSE) was found between the experimental and predicted results. RMSE is defined in Equation 27.

$$RMSE = \sqrt{\frac{\sum_{i=1}^N (EXP(i) - PRED(i))^2}{n}} \quad (27)$$

In Equation 28  $EXP(i)$  is the  $i^{\text{th}}$  experimental data point,  $PRED(i)$  is the  $i^{\text{th}}$  predicted (ACI or CEB-FIB model) data point, and  $n$  is the number of data points.

## DISCUSSIONS

Fig. 2 shows the total shrinkage strain for the three SCC mixes. From this figure it can be seen that SCC20 and SCC40 displayed similar shrinkage strains over the 364 day time period. However, SCC60 had a significantly higher shrinkage strain than the other two SCC

mixes. It is noted that the SCC60 mix had the highest percentage of fly ash replacement at 60% and the highest volume percentage of cement paste at 33%. Therefore, it can be generally concluded that significantly replacing cement with fly ash increases the volume of cement paste resulting in a higher shrinkage strain of SCC. This agrees with previous reports in literature on the significance of cement paste volume on the developed shrinkage strain.

The purpose of this work is to compare the SCC creep to that predicted of similar concretes using the current concrete design models. Here we compare our experimental results to the creep prediction by ACI-209 and CEB-FIP MC-90 creep models. To attempt to model the SCC compression creep experiments with the ACI-209 model, a slump of 300 mm was assumed to model all three mixes. This was done since the ACI model requires the slump to compute creep coefficient. Table 4 shows the RMSE between the ACI model and experimental values. Clearly the ACI model does not accurately predict creep coefficient of SCC20 and SCC40. The model prediction of SCC60 was relatively accurate, however the model still slightly underestimated creep coefficient. It is obvious that the dependence on slump does not allow the ACI-209 model to accurately predict the creep coefficient of SCC.

To account for the inaccuracy of the ACI-209 model's prediction of creep of SCC, a new coefficient was proposed to replace the slump coefficient in calculating the creep coefficient. This new coefficient was based on the fly ash replacement percentage and defined in Equation (15). Fig. 3 shows the prediction of creep coefficient for the three SCC mixes based on this modified ACI model. Clearly, modifying the ACI-209 model based on fly ash percentage allows for a more accurate prediction of creep of SCC containing fly ash. The RMSEs between predicted and experimental values are present in Table 4 and a significant reduction is seen between the modified model ACI model and the ACI model using a slump of 300 mm.

To gain further insight into the creep of SCC, the experimental results were compared to the CEB –FIP MC90-99 model. Since the CEB-FIP model has been proven to be very accurate in modeling creep of concrete, a comparison with the CEB-FIP model should give a good indication of how creep of SCC compares with typical concretes. Fig. 4 shows the MC90 – 99 creep coefficient predictions and the creep coefficients from the compression experiments performed on the three SCC mixes. Clearly, SCC mixes exhibit a higher creep than the MC90 – 99 creep model predicts. The RMSEs (presented in Table 4) were 0.521, 2.103 and 0.931 for SCC20, SCC40 and SCC60 respectively. The RMSE is noticeably high for the SCC40 mix, this might have occurred because the intermediate amount of fly ash (40%) in SCC40 did not have only a significant effect on strength but also changed the microstructure enough to affect viscoelastic properties. These results show that the CEB-FIP model also needs to be modified to allow for more accurate creep predictions of SCC mixes containing fly ash.

## CONCLUSIONS

Comparison of the experimental results with the ACI 209 creep prediction model showed the ACI model to be unable to predict the creep of SCC. It was shown that using maximum slump for SCC mixes was not adequate for creep prediction. Therefore, a modified ACI

model was suggested allowing for the model to more accurately predict the creep coefficient of SCC mixes containing class-F fly ash. The CEB-FIP MC90-99 creep prediction model also underestimated the amount of creep coefficient for all three SCC mixes. The underestimation was most pronounced for the SCC mix with an intermediate amount of class-F fly ash. It is recommended that the MC90-99 model be modified to allow safe prediction of creep of SCC with high amounts of class-F fly ash.

## ACKNOWLEDGEMENTS

The authors would like to extend their upmost gratitude to Kenny Martinez, Eslam Soliman, and Dr. Jung Joong Kim for their efforts in helping casting concrete specimens and recording some of creep experimental measurements.

## REFERENCES

- ACI 209.2R-08. (2008). Guide for Modeling and Calculating Shrinkage and Creep in Hardened Concrete. Farmington Hills, MI, American Concrete Institute.
- Adam, I. (2003). Effect of Age at Loading on Creep of High Performance Concrete. International Conference on Performance of Construction Material in the New Millenium - A New Era of Building, Cairo, Egypt, Elmaarefa Printing House: 1315-1324.
- Adam, I. 2011(a). Properties of Self-Consolidating Concrete Incorporating Different Sand to Aggregate Ratios. Engineering Research Journal **131**: C1-C18.
- Adam, I. 2011(b). Effect of Binder Content on Properties of Different Self-Consolidating Concrete Types. Engineering Research Journal **131**: C19-C37.
- Adam, I., et al. (2007). Creep and Shrinkage of Self-Consolidating Concrete: Preliminary Reults. 12<sup>th</sup> ICSGE Cario, Egypt:1015-1024
- ASTM (2007). ASTM C192/C192M - 07 Standard Practice for Making and Curing Concrete Test Specimens in the Laboratory. West Conshohocken, PA, ASTM International.
- Bouzoubaa, N. and M. Lachemi (2001). Self-Compacting Concrete Incorporating High Volumes of Class F fly Ash - Preliminary Results. Cement and Concrete Research **31**(3): 413-420.
- Brouwers, H. J. H. and H. J. Radix (2005). Self-Compacting Concrete: Theoretical and Experimental Study. Cement and Concrete Research **35**(11): 2116-2136.
- Collepari, M. e. a. (2005). Strength, Shrinkage and Creep of SCC and Flowing Concrete. Second North American Conference on the Design and Use of Self-Consolidating Concrete and the Fourth International RILEM Symposium on Self-Compacting Concrete. Chicago, USA, Hanley-Wood: Addison, Illinois: **911-920**.
- Domone, P. L. (2005). Self-Compacting Concrete: An Analysis of 11 Years of Case Studies Cement & Concrete Composites **28**(2): 197-208.
- Domone, P. L. (2007). A review of the Hardened Mechanical Properties of Self-Compacting Concrete. Cement & Concrete Composites **29**(1): 1-12.
- European Slef-Compacting Concrete Group, (2005). The European Guidelines for Self-Compacting Concrete. BIBM, CEMBUREAU, ERMCO, EFCA and EFNARC.
- Heirman, G., L. Vandewalle, et al. (2008). Time-Dependent Deformations of Limestone Powder Type Self-Compacting Concrete. Engineering Structures **30**(10): 2945-2956.

- Khatib, J. M., (2008) Performance of Self-Compacting Concrete Containing Fly Ash, *Construction and Building Materials* **22**(9): 1963-1971.
- Kayat, K. H. and Long, W. J. (2010) Shrinkage of Precast, Prestressed Self-Consolidating Concrete. *ACI Materials Journal* **107**(3): 231-238.
- Lowke, D. and P. Schießl (2008). Effect of Powder Content and Viscosity Agents on Creep and Shrinkage of Self-Compacting Concrete. Proc. of the Eighth International Conference on Creep, Shrinkage, and Durability of Concrete and Concrete Structures, Ise-Shima, Japan, CRC Press: 655-661.
- Maia, L. M., S. Nunes, et al. (2008). Influence of Paste Content on Shrinkage and Creep of SCC. Proc. of the Eighth International Conference on Creep, Shrinkage, and Durability of Concrete and Concrete Structures, Ise-Shima, Japan, CRC Press: 675-680.
- Mazzotti, C. and C. Ceccoli (2008). Creep and Shrinkage of Self Compacting Concrete: Experimental Behavior and Numerical Model. Proc. of the Eighth International Conference on Creep, Shrinkage, and Durability of Concrete and Concrete Structures, Ise-Shima, Japan: 667-673.
- Neville, A. M., W. H. Dilger, et al. (1983). Creep of Plain and Structural Concrete. New York, NY, USA, Longman Inc.
- Ozawa, K., K. Neakawa, et al. (1989). Development of High-Performance Concrete Based on Durability Design of Concrete Structures. East Asia and Pacific Conference on Structural Engineering and Construction (EASEC-2).
- Persson, B. (2005). Self Consolidating Concrete, High Performance Concrete, and Normal Concrete, Affected by Creep at Different Age, Curing, Load Level, Strength, and Water-Cement Ratio with some Interrelated Properties. *American Concrete Institute Special Publication* **229**: 63-91.
- Reinhardt, A. K., et al. (2008). Total and Basic Creep and Shrinkage of Self-Consolidating Concrete. Third North American Conference on the Design and use of Self-Consolidating Concrete Chicago, Illinois.
- Sahmaran, M., I. O. Yaman, et al. (2009). Transport and Mechanical Properties of Self Consolidating Concrete with High Volume Fly Ash. *Cement & Concrete Composites* **31**(2): 99-106.
- Seng, V. and H. Shima (2005). Creep and Shrinkage of Self-Compacting Concrete with Different Limestone Powder Contents. Second North American Conference on the Design and Use of Self-Consolidating Concrete and the Fourth International RILEM Symposium on Self-Compacting Concrete. Chicago, USA, Hanley-Wood: Addison, Illinois: 981-987.
- Sukumar, B., K. Nagamani, et al. (2008). Evaluation of Strength at Early Ages of Self-Compacting Concrete with High Volume Fly Ash. *Construction and Building Materials* **22**(7): 1394-1401.

**Table 1** Mixture proportions of all concrete mixes used in creep experiments

	w/cm <sup>+</sup>	Weight per unit volume, kg/m <sup>3</sup>					mL/m <sup>3</sup>	
		Water	Cement	Fly Ash	Fine Aggregate	Coarse Aggregate	SP*	VMA**
<b>SCC20</b>	0.33	150	360	90	920	809	7650	4140
<b>SCC40</b>	0.33	150	270	180	902	794	4050	1800
<b>SCC60</b>	0.33	150	180	270	886	779	4500	1800

+ cm: cementitious content,  
 \* SP: superplasticizer  
 \*\* VMA: viscosity modifying agent

**Table 2** Fresh properties of all concrete mixes used in creep experiments

	Slump flow (mm)	T <sub>500</sub> time (s)	Passability (%)
<b>SCC20</b>	810	4.0	96
<b>SCC40</b>	710	4.0	93
<b>SCC60</b>	840	3.0	---

**Table 3** Hardened concrete properties

	7 day Compressive Strength (MPa)	28 day Compressive Strength (MPa)
<b>SCC20</b>	34.6 ± 2.2	42.6 ± 3.0
<b>SCC40</b>	13.9 ± 2.0	28.9 ± 8.4
<b>SCC60</b>	12.2 ± 1.0	19.7 ± 0.6

**Table 4** Root Mean Square Error (RMSE) of ACI model, modified ACI model, and the CEB-FIB model

	RMSE		
	ACI	Modified ACI	CEB-FIP
<b>SCC20</b>	1.174	0.449	0.521
<b>SCC40</b>	1.183	0.889	2.103
<b>SCC60</b>	0.476	0.346	0.931

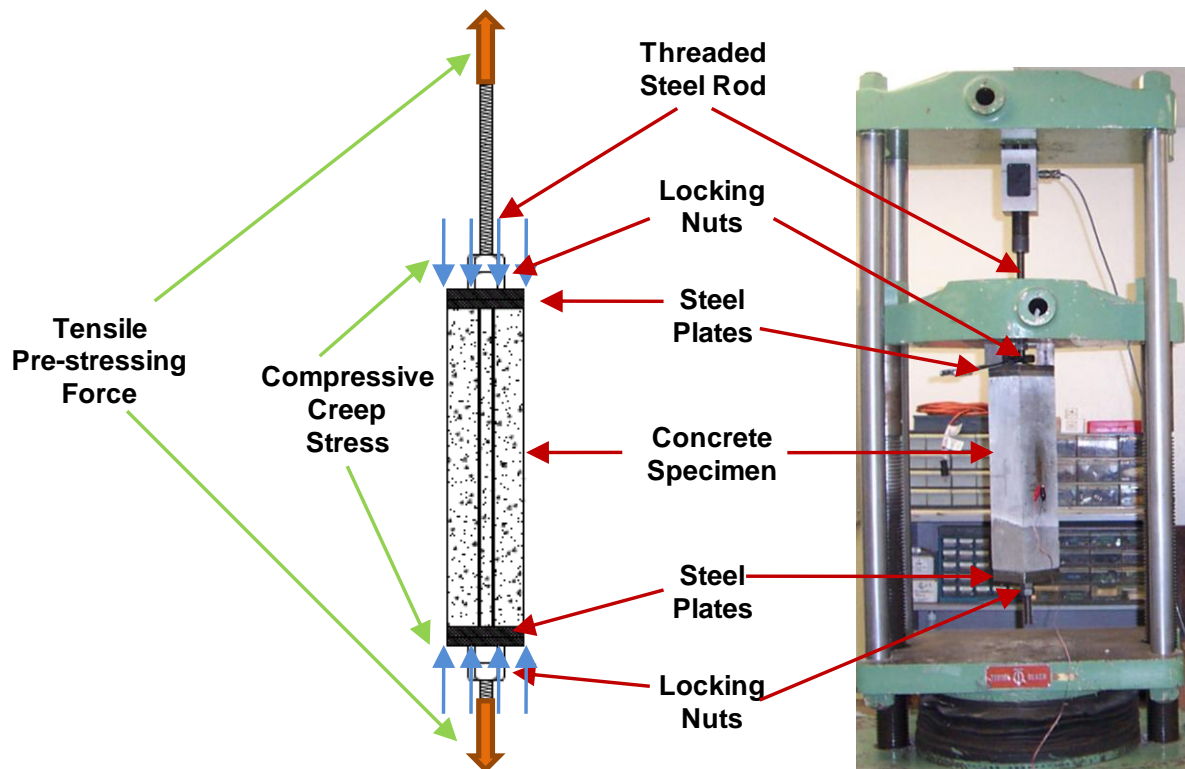


Fig. 1 Concrete creep frame loaded in universal testing machine and stress transfer schematic

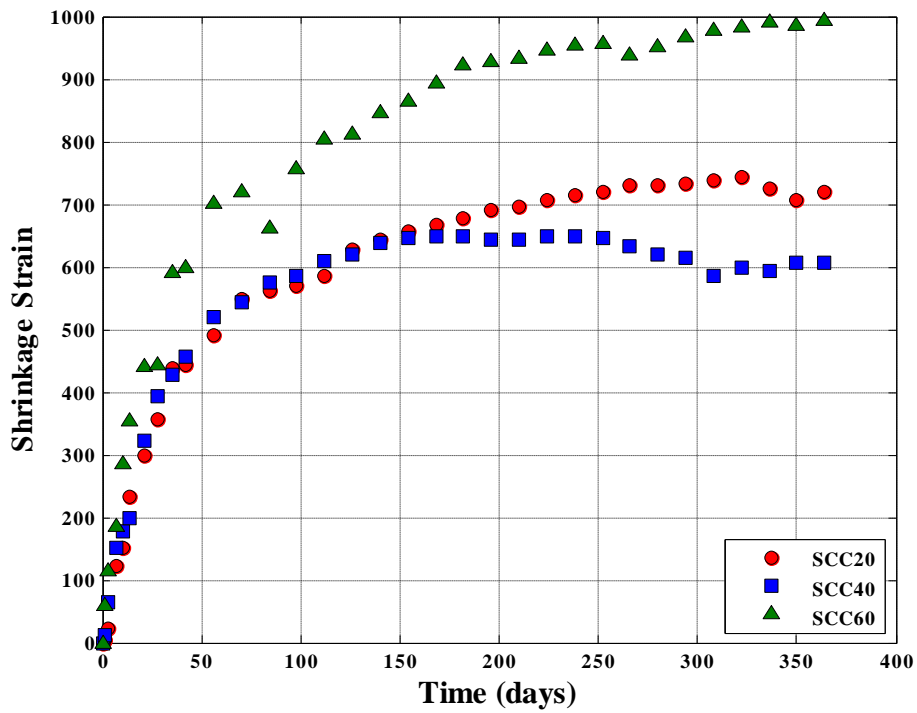
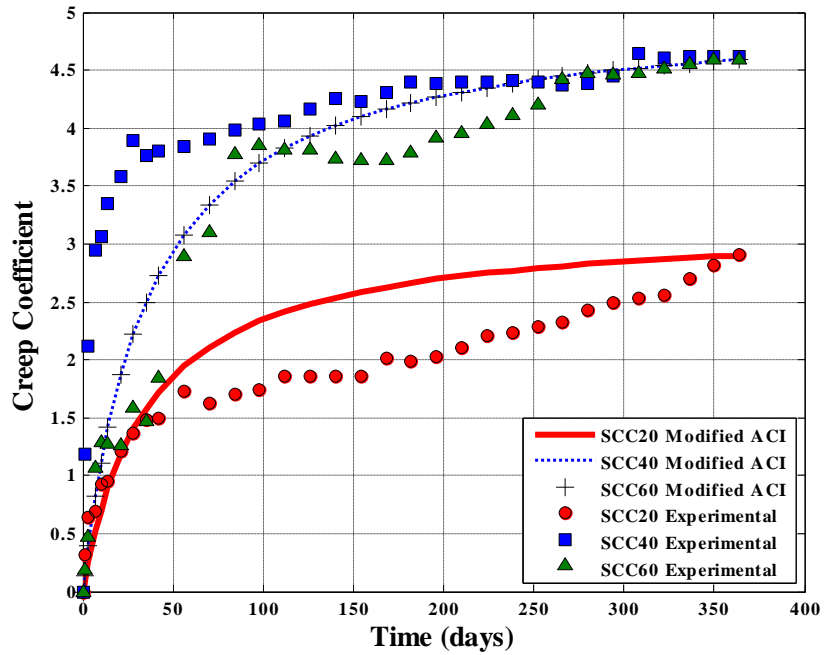
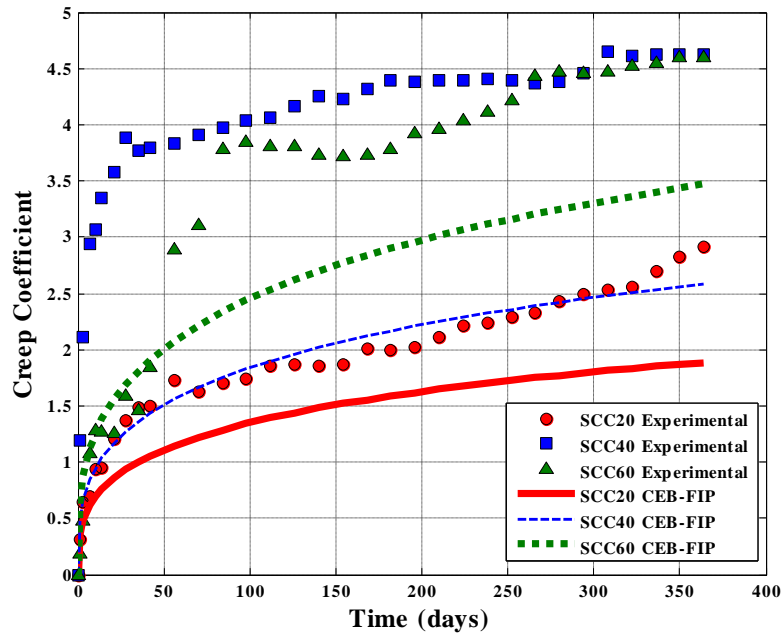


Fig. 2 Shrinkage strain for all SCC mixes tested in experiments



**Fig. 3** Experimental vs. ACI modified predicted creep coefficients for SCC with different Fly ash contents.



**Fig. 4** Experimental vs. CEB-FIP predicted creep coefficients for SCC with different Fly ash contents.